Environmental Engineering and Management Journal

August 2019, Vol. 18, No. 8, 1755-1763
http://www.eemj.icpm.tuiasi.ro/; http://www.eemj.eu

"Gheorghe Asachi" Technical University of Iasi, Romania

NEW TiO_2-Ag NANOPARTICLES USED FOR ORGANIC COMPOUNDS DEGRADATION

Consuelo Gómez de Castro[1], Cătălina Nuţescu Duduman[2], Maria Harja[2*], Doina Lutic[3], Tatjana Juzsakova[4], Igor Creţescu[5*]

[1]Complutense University of Madrid, Faculty of Chemical, Department of Materials and Chemical Engineering, Av. Séneca, 2, 28040 Madrid, Spain
[2]"Gheorghe Asachi" Technical University of Iasi, Faculty of Chemical Engineering and Environmental Protection, Chemical Engineering Department, 73 Prof.dr.doc. Dimitrie Mangeron Street, 700050 Iasi, Romania
[3]"Alexandru Ioan Cuza" University of Iasi, Blvd. Carol I No 11, 700506 Iaşi, Romania
[4]University of Pannonia, 10 Egyetem St. Veszprém, 8200 Hungary
[5]"Gheorghe Asachi" Technical University of Iasi, Faculty of Chemical Engineering and Environmental Protection, Department of Environmental Engineering and Management, 73 Prof.dr.doc. Dimitrie Mangeron Street, 700050 Iasi, Romania

Abstract

TiO_2-assisted photocatalysis is used in numerous environmental applications and for the manufacturing of different products. Ag-doped TiO_2 nanoparticles were synthesized by impregnation using silver nitrate solution on TiO_2 obtained by sol-gel method and on commercial Degusa P25 (Evonik). Silver is widely studied as a dopant for semiconductor materials, due to its antibacterial properties. In addition to this, it acts as electron sink and donor for photogenerated electrons, enhancing the photocatalytic activity. The physical properties of the samples calcined at different temperatures were investigated by XRD, XRF, SEM, TEM, SAED and EDAX techniques. The calcination temperature of 650°C led to the total transformation of titanium dioxide (anatase) to rutile phase when commercial P25 was doped with Ag. In the case of samples produced by sol-gel method, the anatase is still the major phase even at this temperature. The photocatalytic activity of the synthesized catalysts was evaluated in the UV-assisted photodegradation of Rhodamine 6G and Congo Red dyes. The conversion yield of Rhodamine 6G reached 66.5% and that of Congo Red was 53% after 120 minutes of irradiation.

Key words: photocatalysis, photodegradation, silver, titanium oxide

Received: September, 2018; Revised final: January, 2019; Accepted: April, 2019; Published in final edited form: August, 2019

1. Introduction

During the past years, the nanomaterials have attracted high interest in research and practical implementations, due to their special and interesting properties. The most common applications concern their use as adsorbents, (photo) catalysts, magnetic materials, ceramics, drug carriers, semiconductors, biomaterials etc. Considering also the specific properties related to nanoscale structure, the nanomaterials are often remarkable for their high photocatalytic performances, easy availability, stability in time, low toxicity etc.

The synthesis of nanocomposites by doping with noble metal nanoparticles (Pt, Pd, Au and Ag) was employed to modify semiconductors as TiO_2, ZnO, CuO, Bi_2WO_6, $La_2Ti_2O_7$ (Favier et al., 2016; Lutic et al., 2017; Ma et al., 2018, Mahmoodi et al., 2017) aiming to improve their behavior in the photocatalytic reactions. Due to the good electron collection/transport abilities and UV response properties of titanium dioxide and noble metal

* Author to whom all correspondence should be addressed: e-mail: icre@tuiasi.ro; mharja@tuiasi.ro

nanoparticles, these nanocatalysts exhibit combined or synergistic effects in enhancing their individual performances in many photocatalytic applications (Cantarella et al., 2016; Qian et al., 2018; Zhao et al., 2016).

The photocatalysts derived from titanium dioxide are extensively used due to their convenient band gap value, chemical and thermal stability, good photocatalytic activity, low cost etc. (Djoki et al., 2012; Ivanova et. al., 2013; Liu et al., 2017).

Titanium dioxide exists in three main polymorphs: rutile, anatase and brookite. Anatase and rutile are the most common for the photocatalytic applications, having band gap values of 3.23 and 3.02 eV respectively. The electron promotion from the valence band to the conduction band can be promoted by UV and visible radiation (Tobaldi et al., 2013). This is a premise for the oxidative degradation of persistent organic compounds in aqueous media, in the presence of photocatalytic solids activated by light. The photocatalytic activity is highly increased by the incorporation of noble metals nanoparticles in semiconductive oxides (Guo et al. 2009; Lee et al., 2005; Liu et al., 2004). Noble metals as Pt, Pd, Au, Ag can be used for TiO_2 doping, because they increase the photocatalytic activity, by avoiding the recombination of electron-hole pair (He et al., 2013; Ran et al., 2018, Sarina et al., 2013). On the other part, silver is a noble metal with exceptional antibacterial performance. Silver nanoparticles exhibit numerous applications: it acts as a disinfection agent in biomedicine, where it is used in various therapies, as catalyst in photovoltaic applications and chemical sensing (Sanzone et al., 2018). Silver nanoparticles are usually prepared by the chemical reduction of a silver salts.

The sol-gel method is a simple and effective technique to be used for obtaining various new TiO_2 nanoparticles with controlled properties (Nutescu Duduman et al., 2016, 2018). The impregnation method is a convenient, simple and cheap way to introduce noble metals into the oxide structures, with good dispersion of the metal on the surface of the parent oxide (Van Dillen et al., 2003).

The formation of titanium dioxide by sol-gel method generally comprises the use of a titanium organic salt via hydrolysis with the formation of Ti – OH groups, followed by the condensation step, when bonding of the titanium species by oxo (Ti – O – Ti) and hydroxo (Ti – OH – Ti) bridges occurs, by progressive and finally deep elimination of water molecules (Galkina et al., 2011). The TiO_2-Ag photocatalyst with controlled metal particle size can be obtained by the sol-gel and impregnation methods (Amin et al., 2009; Guo et al. 2009). The TiO_2-Ag nanocatalysts are cost-effective, efficient, environmentally friendly and highly efficient catalysts for the oxidation of organic compounds from wastewaters (Harja et al., 2018; Hussain et al., 2016).

The photocatalytic activity of TiO_2 is influenced by several factors: the nature of the crystalline phase, the crystallinity degree, the particle size, the nature and dispersion degree of the doping species etc. (Hu et al., 2017; Lutic et al., 2018; Vajda et al., 2016).

Many stable organic compounds are widely used in pharmaceutical production, textile treatments and dyeing, plastic and rubber manufacturing and several industrial processes (Harja et al., 2017; Khalik et al., 2018). These processes have a strong impact on the environment, since the use of water is ubiquitous and the formation of wastewaters contaminated with stable and dangerous species represents a continuous problem (Ciobanu et al., 2013; Harja et al., 2011; Harja et al., 2016; Harja and Ciobanu, 2018). The advanced recovery and/or destruction of organic compounds from wastewaters became a priority in the last decades. The constant increasing demand for water and, therefore, the higher wastewater production with hardly degradable pollutants generates severe environmental problems (Ciobanu et al., 2014; Rusu et al., 2014).

Rhodamine 6 G (R6G) and Congo Red (CR) are organic compounds with complex structures, which can be used as model molecules in the research aiming at to test new materials as adsorbents and photocatalysts with applications in the advanced wastewater treatment (Bhakya et al., 2015; Ghazzal et al., 2012; Lutic and Cretescu, 2016; Lutic et al., 2012).

In this work, we have synthesized TiO_2-Ag nanocomposites by the sol-gel method from titanium tetra-isopropoxide and silver nitrate and compared its photocatalytic performance with a sample prepared by the wet impregnation of commercial titanium dioxide P25 with silver nitrate. The samples were characterized by XRD, XRF, SEM and TEM and tested in the UV-assisted photocatalytic degradation of R6G and CR dyes from aqueous solutions simulating wastewaters. The decomposition yield of Rhodamine 6G reached 66.5 % in 120 minutes, while Congo Red conversion was 53 % under the same period of time.

2. Experimental part

2.1. Sample preparation

Titanium tetraisopropoxide (TIP), Panreac was used as TiO_2 nanoparticles precursor. Titanium dioxide P25 (Degussa) was used for the experiments without any purification procedure and silver nitrate ($AgNO_3$, Sigma Co.) was used for Ag doping. The sol-gel synthesis under acidic conditions was employed for the preparation of TiO_2 nanoparticles, following a procedure reported in a previous work (Nutescu Duduman et al., 2018), using nitric acid as a hydrolysis-condensation ratio potentiation. The sample was further treated with silver nitrate solution, ammonia and hydrazine, to complete the hydrolysis and precipitation. Thus, reduced Ag on the TiO_2 nanoparticles was obtained. The chemicals ratios were chosen to allow obtaining an 1/10 weight ratio of Ag/TiO_2. The sample was dried at 110°C overnight (labelled as Ag_TiO_2). Half of the sample was used as-synthesized in the photocatalytic tests and half was

thermally activated. The activation was carried out by calcination at 650°C for 2 hours (heating rate of 1°C min^{-1}) (labelled as Ag_TiO_2 Calc 650).

The sample based on commercial titanium dioxide P25 was prepared by incipient wetness impregnation (IWI) with $AgNO_3$ solution prepared in water and ethanol. The recipe was adjusted to provide the same 1/10 weight ratio between Ag and TiO_2 particles as in the case of the sol-gel method. The P25 powder (2 g) was dried for 2 hours at 200°C in a crucible. The $AgNO_3$ solution was prepared in the proper amount of water allowing the complete dissolution according to the salt solubility, then ethanol was added to reach a solution volume of 3 mL. The $AgNO_3$ solution was rapidly poured onto the hot P25 powder and the crucible was covered to avoid the powder spreading. The sample was let to cool down to room temperature and then dried at 100 °C for several hours. The sample activation was made for half of the powder amount at 500°C (labelled as Ag_P25 Calc 500) and for the other half at 650°C (labelled as Ag_P25 Calc 650), heating rate of 1°C min^{-1}, for 2 hours.

The morphology and the chemical composition of the sample were determined by SEM–EDAX analysis, by using JEOL 6400 apparatus with Oxford Link EDAX microanalyser and Pentafet light sensing with coupled EDSX-max (Oxford Instruments) device. The elements concentrations were obtained by averaging the individual values of five parallel determinations at different points. X-ray diffraction (XRD) patterns were obtained on a Shimadzu D6000 apparatus, in the range 5–80 °(2 theta), under CuKα radiation (λ = 1.5406 Å). X-Ray Fluorescence (XRF) is the emission of characteristic secondary fluorescent X-rays from a material having been excited by bombardment with high-energy X-rays or gamma rays. The two expecting elements (Ag and Ti) were monitored and analyzed by this procedure for each sample. The samples were scanned two times for 60 s each. The investigation of the porous structure was performed by BET nitrogen adsorption at 77K, on a Nova 2200e machine.

2.2. Photocatalytic activity

The photocatalytic degradation was performed in a 500 mL cylinder glass reactor, equipped with a central quartz tube hosting an Osram UV-A lamp of 9W. Details about this setup are available elsewhere (Lutic et al., 2012). The stirring was made magnetically. During the photocatalytic run, an aluminum foil was wrapped around the reactor several times to protect the operator, as well as to keep as much as possible the UV irradiation inside the ring-shaped reaction space between the reactor body and the lamp's tube. The solutions were prepared by using deionized water. The pH value during the reactions was the native value of the dye. Before the photocatalytic run, the photocatalyst powder was finely grounded, dispersed in the dye solution and stirred for 30 min in dark at room temperature, in order to allow reaching the adsorption/desorption equilibrium. The moment when the UV lamp was turned on after achieving the adsorption equilibrium was counted as zero-time. Samples of approximately 4 mL were withdrawn after defined time durations (0, 5, 10, 15, 30, 45, 60, 90 and 120 min), filtered through 0.45 μm syringe filter and analyzed by spectrophotometry, for measuring the remaining dye concentration. All the experiments were carried out at ambient temperature.

The concentrations of the organic compounds were measured based on the intensity of the characteristic peaks from the visible range of the UV–Vis spectra, obtained on a Shimadzu UV-1700 spectrophotometer, in 1 cm optical length plastic cuvettes. If the absorbance values were higher than the limits used in the calibration curves obeying the Lambert-Beer law, the solutions were diluted accordingly before the measurements. The dye R6G concentrations for the tests were comprised between 15-65 ppm and the tests with dye CR were made at 40 ppm concentration.

The efficiency of the photocatalyst was quantified as the degree of the dye conversion calculated with the Eq. (1):

$$Conversion(\%) = \frac{C_0 - C_t}{C_0} \cdot 100 \quad (1)$$

where: C_o and C_t are, respectively, the initial dye concentrations and the dye concentrations measured at time t (ppm).

3. Results and discussion

3.1. Sample characterization

The XRD analysis was used for the identification of the crystalline structure of the samples and the evaluation of the solids phase purity. The XRD diffraction patterns are given in Fig. 1.

The samples Ag_TiO_2 Calc 650 and Ag_P25 Calc 500 mainly consist of anatase phase, as shown by the peaks due to the following characteristic planes and corresponding 2θ angles: (101), 25.5°; (004), 38.8°; (200), 48.1°; (105), 53.7° and (204), 62.8° (Sakurai and Mizusawa, 2010). The sample Ag_TiO_2 also contains anatase phase, but its peaks have much lower intensity and higher half height width than that of the calcined sample, indicating the formation of smaller particles and lower crystallinity degree. The main peaks assigned to rutile phase due to the following planes and 2θ angles of (110), 27.4°, (101), 36°, (200), 39.5°, (111), 41.2°, (210), 44.2°, (211), 54.3° and (220), 56.6° appear in the pattern of sample Ag_P25 Calc 650. This indicates that it consists of almost pure rutile (Wetchakun et al., 2012). The sample Ag_P25 Calc 500 is a mixture of anatase and rutile, as in the parent P25 powder. The metallic silver displays peaks at 38.2; 45 and 63° owning to planes of (111), (200) and (222) (Waterhouse et al., 2001). The

peaks due to silver and silver oxides at 2θ of 38° and 63° partly overlap with the maxima of anatase, therefore the peak at 2θ angles of 45° could be considered the main indication for the presence of important amounts of silver deposited as an individual phase on titanium dioxide. This peak cannot be seen on the XRD pattern of sample Ag_TiO_2, due probably to the weak crystallization degree and very small particle size. The XRF study allowed to determine the chemical composition of the samples surface. The results are displayed in Table 1.

During the high calcination temperature process, the silver concentration on the surface decreases from an average of 9.87 % (calcination at 500°C) to 6.34 % (calcination at 650°C), while the titanium concentration increases correspondingly. This is due to the increase in silver particle size (as see in the TEM images, Fig. 2).

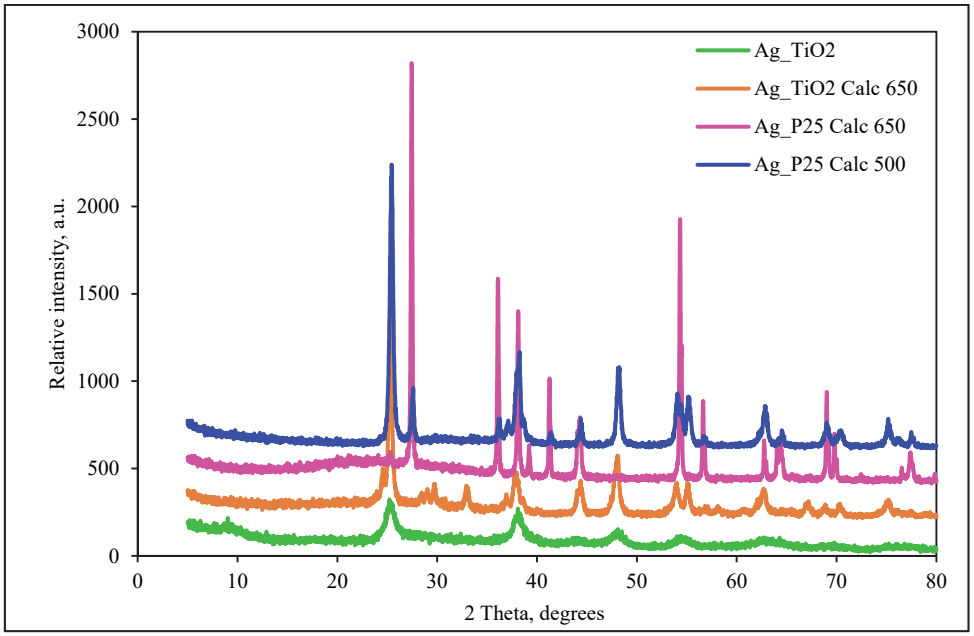

Fig. 1. XRD patterns of Ag_TiO_2 based samples

Table 1. Chemical composition and BET specific surface areas values

Sample label	***Ag***	***Ti***	***BET specific surface area, $m^2 g^{-1}$***
Ag_TiO_2	-	-	7.8
Ag_TiO_2 Calc 650	6.34±0.48	54.88±0.38	6.9
Ag_P25 Calc 500	9.87±0.06	52.40±0.37	30.0
Ag_P25 Calc 650	-	-	7.3

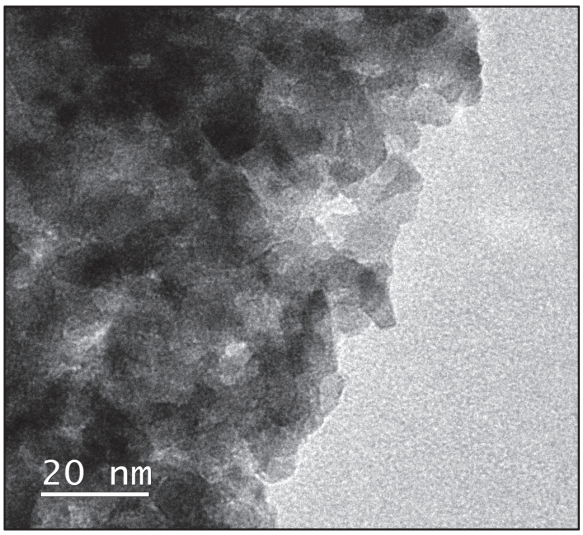

(a)

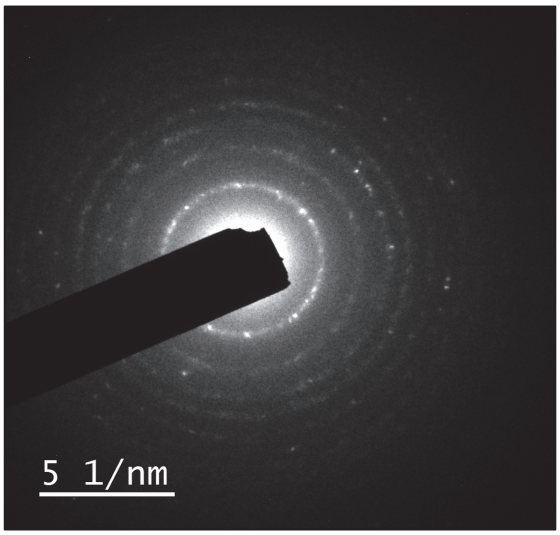

(b)

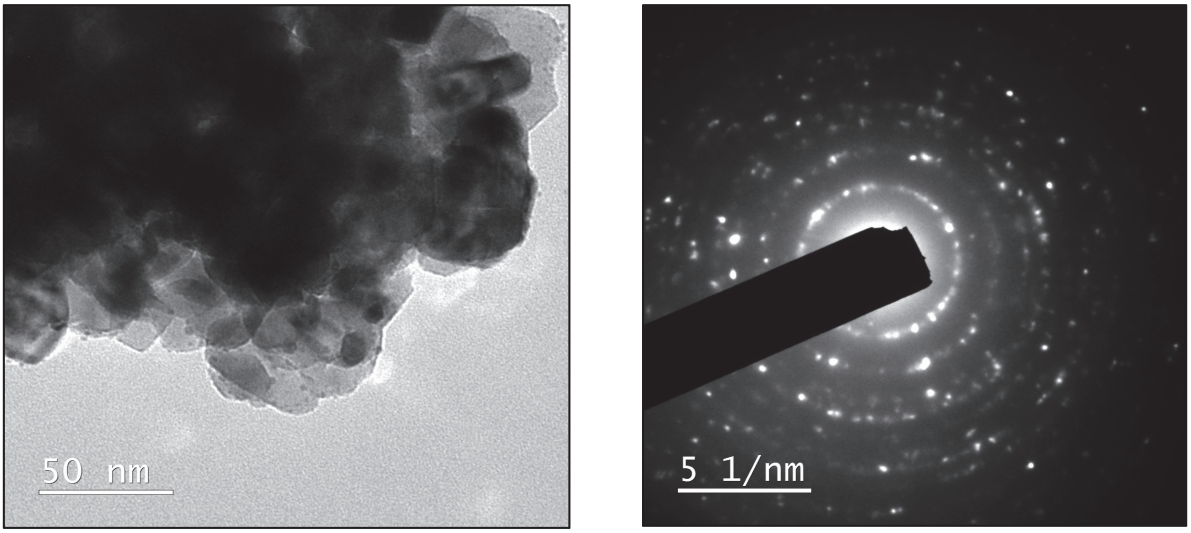

(c) (d)

Fig. 2. TEM analysis for samples: Ag_TiO_2-(a) TEM and SAED (b) image; Ag_TiO_2 Calc 650- (c) TEM and SAED image (d)

The values of the BET surface areas for all the samples are rather low (except the sample Ag_P25 Calc 500), indicating that the structure of the solids is rather compact (Table 1).

The TEM analysis of the samples (Fig. 2) indicates that the crystallization degree of the sample Ag_TiO_2 Calc 650 during the thermal treatment becomes significantly higher than in the uncalcined sample Ag_TiO_2, as shown by the strong light spots from the SAED image.

The silver particles can be seen as dark dots of about 5-7 nm only in the calcined samples, confirming the outcome of the interpretation of the XRD patterns.

3.2. Photocatalytic performance

The behavior of the samples as photocatalysts was investigated in the oxidative decolorization of Rhodamine 6G (R6G) and Congo Red (CR) dyes. The chemical structures of the dyes are shown in Fig. 3.

The samples Ag_TiO_2 and Ag_TiO_2 Calc 650 were used at a dose of 1 g/L, while the P25 based samples were tested at 0.5 g/L. The particle sizes of P25 are very small, therefore the turbidity of the photocatalyst suspension is too high to allow the radiation to pass through the complete dye solution volume in the photoreactor.

The R6G concentration was measured by the intensity of the main peak showing up in the visible region of the UV-Vis spectrum at 525 nm. The experiments carried out with dye R6G and the spectra registered during the irradiation up to 120 minutes are given in Fig. 4.

The spectra show a constant decrease of the main peak from the visible region of the spectrum, while the peak around 230 nm from the UV region of the spectrum increases gradually due to the nitrate anion formation due to the oxidation of the amine group. This is an indication that the decomposition reaction splits the dye molecule into smaller fragments, however, this did not result in complete mineralization.

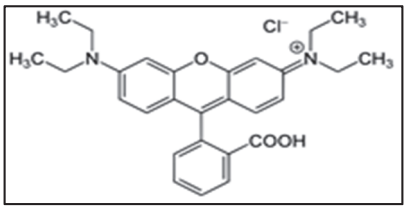

(a)

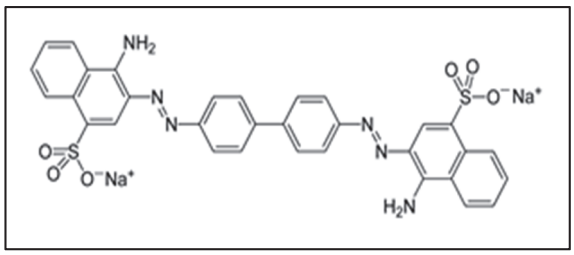

(b)

Fig. 3. Rhodamin 6G (a) and Congo Red (b) chemical structures

An experiment performed as a reference using P25 as photocatalyst on a R6G solution of 30 ppm gave a conversion degree of only 23% after 120 minutes. However, the photocatalyst-solution suspension was very turbid and therefore, the irradiation eficiency in the whole volume must have been viciated due to the shielding.

The calcination temperature has a tremendous influence on the thermodynamic stability of the crystalline phases of TiO_2. The literature mentions that, depending on the preparation procedure and/or dopants, the transformation of anatase to rutile phase occurs at temperature values comprised between 600-800°C (Hanaor and Charles, 2011; Su et al. 2011). The

photocatalytic activity is related to the formation of the electron-hole pair on the influence of irradiation and on the delay of their recombination, which occur in high yields on anatase-rutile mixtures, while pure rutile is inactive, despite its convenient band gap value of 3.02 eV (Atitar et al., 2015). This fact was confirmed by our experiments: on the sample Ag_P25 Calc 650 which transformed totally into rutile phase by calcination, as shown by the XRD pattern, the photodegradation of dye R6G did not occur at all. The behavior of the sample obtained from TIP was noticeably different: the anatase remains the main phase even if the calcination was carried out at 650°C. The remaining organic phase and the presence of silver stabilized in high extent resulted in the hindrance of the transformation of the anatase phase into rutile. Several researchers, as reviewed by Hanaor and Sorrell (2011) had reported this behavior. The interesting behavior from the point of view of phase stability of sample Ag_TiO_2 Calc 650 motivated us to test it in several experiments, in order to explore its adsorptive and photocatalytic potential. Therefore, several R6G concentrations between 15-65 ppm were used to test its performance. The conversion values for different initial dye concentrations and irradiation time values are shown in Fig. 5. The results indicate, as expected, that the extent of dye decolorization is higher in case of the lower initial concentration values. After 60 min of irradiation, the decolorization was over 52%, while additional 1 h time-on-stream resulted only a conversion degree of 66.5%. Even the decolorization degree values was not very high, for all the initial concentration values, a constant increase of the decolorization was observed in time. The preparation method did not support the formation of a porous structure, therefore the initial dye uptake by adsorption reached only 11-16 % at all the concentation values tested.

The behavior of the photocatalysts in the decomposition of Congo Red dye was consistently different than in case of dye R6G. The decolorization was quantified by measuring the absorbance at the characteristic wavelength of 497 nm. An example of the UV-Vis spectra evolution in time for the decomposition of dye CR is shown in Fig. 6.

Both preparations Ag_TiO_2 and Ag_TiO_2 Calc 650 were totally inactive for the conversion of this dye. In turn, very similar behaviors between the samples Ag_P25 calc 500 and Ag_P25 Calc 650 were noticed (Fig. 7).

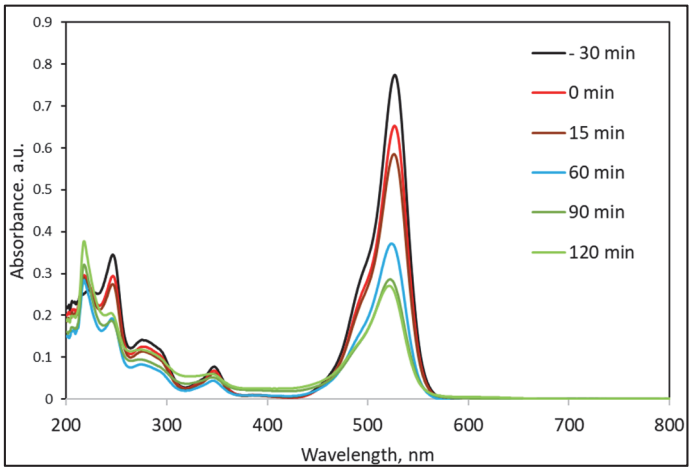

Fig. 4. R6G spectra during the photocatalytic test (catalyst: Ag_TiO_2 Calc 650, initial dye concentration 15 ppm, photocatalyst dose: 1 g/L)

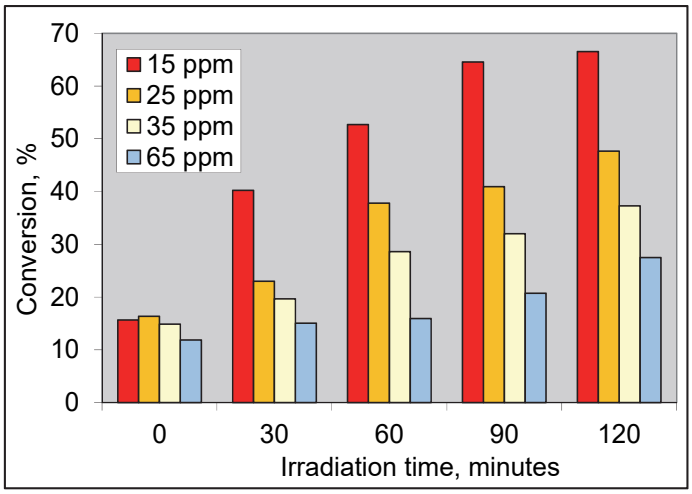

Fig. 5. Conversion degrees on sample Ag_TiO_2

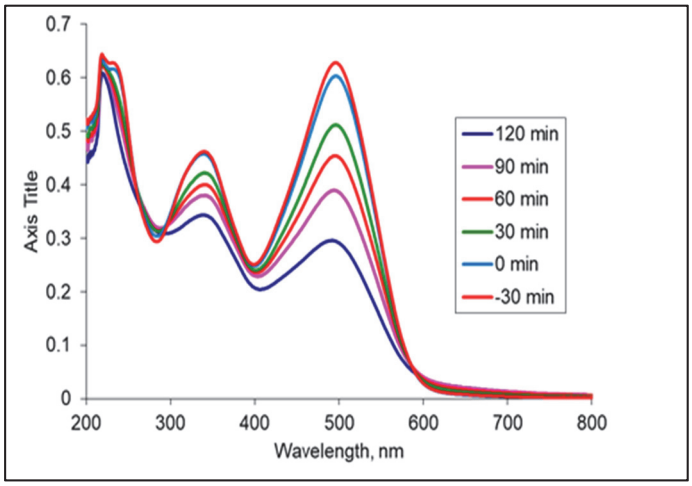

Fig. 6. Evolution of UV-Vis spectra of CR during the photocatalytic decomposition (sample Ag_P25 Calc 500, 0.5 g/L photocatalyst, 40 ppm initial dye concentration)

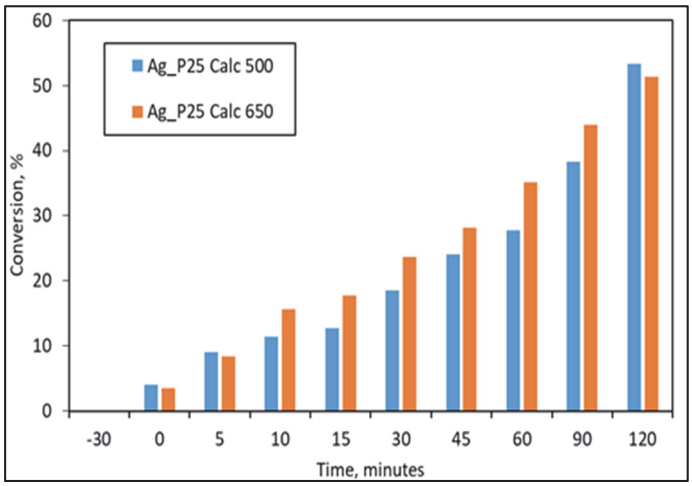

Fig. 7. CR photocatalytic decomposition on P25 based samples

4. Conclusions

In this paper a simple sol-gel method was described for obtaining Ag-doped TiO_2 nanoparticles. Titanium isopropoxide was hydrolyzed with nitric acid, precipitated by ammonia solution, doped with silver nitrate and reduced with hydrazine to silver. The samples used for comparison were prepared by incipient wetness impregnation of P25 commercial titanium dioxide with silver nitrate. The activation of the samples was made at 650°C.

The XRD analysis indicated that anatase was the main phase for the sample prepared by sol-gel method, even if the calcination temperature was 650°C. For the sample prepared from P25 commercial titanium dioxide, rutile was the only phase at this activation temperature. The TEM images confirm the incorporation of silver as distinctive grains on the surface of the calcined sample.

The photocatalytic decomposition tested by using Rhodamine 6G (R6G) and Congo Red (CR) as test compounds highlighted very different behaviors. The dye R6G was decomposed up to a yield of 66.5% on the sol-gel prepared sample, activated at 650°C. The dye CR was decolorized in turn only in the presence of the P25 based solid.

Acknowledgements

The authors are grateful for the partial support of this work by the Ministry of Economy and Competitiveness from Spain, Reference: MAT2013-46755-R, and grant POSDRU/159/1.5/S/133652.

References

Amin A.S., Pazouki M., Hosseinnia A., (2009), Synthesis of TiO_2–Ag nanocomposite with sol–gel method and investigation of its antibacterial activity against *E. coli*, *Powder Technology*, **196**, 241-245.

Atitar M.F., Ismail A.A., Al-Sayari S.A., Bahnemann D., Afanasev D., Emeline A.V., (2015), Mesoporous TiO_2 nanocrystals as efficient photocatalysts: Impact of calcination temperature and phase transformation on photocatalytic performance, *Chemical Engineering Journal*, **264**, 417-424.

Bhakya S., Muthukrishnan S., Sukumaran M., Muthukumar M., Senthil Kumar T., Rao M.V., (2015), Catalytic degradation of organic dyes using synthesized silver

nanoparticles: a green approach, *Journal of Bioremediation & Biodegradation*, **6**, 1-9.

Cantarella M., Sanz R., Buccheri M.A., Ruffino F., Rappazzo G., Scalese S., Privitera V., (2016), Immobilization of nanomaterials in PMMA composites for photocatalytic removal of dyes, phenols and bacteria from water, *Journal of Photochemistry and Photobiology A: Chemistry*, **321**, 1-11.

Ciobanu G., Harja M., Rusu L., Mocanu A.M., Luca C., (2014), Acid Black 172 dye adsorption rom aqueous solution by hydroxyapatite as low-cost adsorbent, *Korean Journal of Chemical Engineering*, **31**, 1021-1027.

Ciobanu G., Ilisei S., Harja M., Luca C., (2013), Removal of Reactive Blue 204 dye from aqueous solutions by adsorption onto nanohydroxyapatite, *Science of Advanced Materials*, **5**, 1090-1096.

Djoki V.R., Marinkovic A.D., Mitric M., Uskokovic P.S., Petrovic R.D., Radmilovic V.R., Janackovic D.T., (2012), Preparation of TiO_2/carbon nanotubes photocatalysts: the influence of the method of oxidation of the carbon nanotubes on the photocatalytic activity of the nanocomposites, *Ceramics International*, **38**, 6123-6129.

Favier L., Harja M., Simion A.I., Rusu L., Kadmi Y., Pacala M.L., Bouzaza A., (2016), Advanced Oxidation Process for the Removal of Chlorinated Phenols in Aqueous Suspensions, *Journal of Environmental Protection and Ecology*, **17**, 1132-1141.

Galkina O.L., Vinogradov V.V., Agafonov A.V., Vinogrado A.V., (2011), Surfactant-Assisted Sol-Gel Synthesis of TiO_2 with Uniform Particle Size Distribution, *International Journal of Inorganic Chemistry*, **2011**, 1-8.

Ghazzal M.N., Kebaili H., Joseph M., Debecker D.P., Eloy P., De Coninck J., Gaigneaux E.M., (2012), Photocatalytic degradation of Rhodamine 6G on mesoporous titania films: Combined effect of texture and dye aggregation forms, *Applied Catalysis B: Environmental*, **115-116**, 276-284.

Guo G., Yu B., Yu P., Chen X., (2009), Synthesis and photocatalytic applications of Ag/TiO_2-nanotubes, *Talanta*, **79**, 570-575.

Hanaor D.A., Sorrell C.C., (2011), Review of the anatase to rutile phase transformation, *Journal of Materials Science*, **46**, 855-874.

Harja M., Barbuta M., Rusu L., Munteanu C., Buema G., Doniga E., (2011), Simultaneous removal of Astrazone blue and lead onto low cost adsorbents based on power plant ash, *Environmental Engineering and Management Journal*, **10**, 341-347.

Harja M., Ciobanu G., (2018), Studies on adsorption of oxytetracycline from aqueous solutions onto hydroxyapatite, *Science of the Total Environment,* **628-629**, 36-43.

Harja M., Ciobanu G., Favier L., Bulgariu L., Rusu L., (2016), Adsorption of crystal violet dye onto modified ash, *Bulletin of the Polytechnic Institute from Iaşi. Chemistry and Chemical Engineering Section*, **62**, 27-37.

Harja M., Kotova O., Samuil C., Ciocinta R., Ciobanu G., (2017), Adsorption of direct green 6 dye onto modified power plant ash, *Agronomy Series of Scientific Research/Lucrari Stiintifice Seria Agronomie*, **60**, 15-20.

Harja M., Sescu A.M., Favier L., Lutic D., Ciobanu G., (2018), *Photodegradation of Rhodamine 6G in Presence of Ag/TiO_2 Photocatalyst*, Intern. Symp. *The Environment and the Industry*, SIMI 2018*,* Proceedings Book, Section Sustainable Environmental Technologies, doi: http://doi.org/10.21698/simi.2018.fp12.

He Y., Basnet P., Murph S.E.H, Zhao Y., (2013), Ag nanoparticle embedded TiO_2 composite nanorod arrays fabricated by oblique angle deposition: toward plasmonic photocatalysis, *ACS Applied Materials & Interfaces*, **5**, 11818-11827.

Hu J., Cao Y., Wang K., Jia D., (2017), Green solid-state synthesis and photocatalytic hydrogen production activity of anatase TiO_2 nanoplates with super heat-stability, *RSC Advances*, **7**, 11827-11833.

Hussain M., Tariq S., Ahmad M., Sun H., Maaz K., Ali G., Zahid Hussain S., Iqbal M., Karim S., Nisar A., (2016), Ag-TiO_2 nanocomposite for environmental and sensing applications, *Materials Chemistry and Physics*, **181**, 194-203.

Ivanova T., Harizanova A., Koutzarova T. Vertruyen B., (2013), Optical and structural characterization of TiO_2 films doped with silver nanoparticles obtained by sol-gel method, *Optical Materials*, **36**, 207-213.

Khalik W.F., Ong S.A., Ho L.N., Wong Y.S., Yusoff N.A., Ridwan F., (2018), Comparison on solar photocatalytic degradation of Orange G and new coccine using zinc oxide as catalyst, *Environmental Engineering and Management Journal*, **17**, 391-398.

Lee M.S., Hong S.S., Mohseni M., (2005), Synthesis of photocatalytic nanosized TiO_2–Ag particles with sol–gel method using reduction agent, *Journal of Molecular Catalysis A: Chemical*, **242**, 135-140.

Liu S.X., Qu Z. P., Han X.W., Sun C.L., (2004), A mechanism for enhanced photocatalytic activity of silver-loaded titanium dioxide, *Catalysis Today*, **93**, 877-884.

Liu X., Bi Y., (2017), In situ preparation of oxygen-deficient TiO_2 microspheres with modified {001} facets for enhanced photocatalytic activity, *RSC Advances*, **7**, 9902-9907.

Lutic D., Coromelci C.G., Juzsakova T., Cretescu I., (2017), New mesoporous titanium oxide-based photoactive materials for the removal of dyes from wastewaters, *Environmental Engineering and Management Journal*, **6**, 801-807.

Lutic D., Coromelci-Pastravanu C., Cretescu I., Poulios I., Stan C.D., (2012), Photocatalytic Treatment of Rhodamine 6G in Wastewater Using Photoactive ZnO, *International Journal of Photoenergy*, **2012**, 1-8.

Lutic D., Cretescu I., (2016), Optimization Study of Rhodamine 6G Removal from Aqueous Solutions by Photocatalytic Oxidation, *Revista de Chimie (Bucharest)*, **67**, 134-138.

Lutic D., Petrovschi D., Ignat M., Creţescu I., Bulai G., (2018), Mesoporous cerium-doped titania for the photocatalytic removal of persistent dyes, *Catalysis Today*, **306**, 300-309.

Ma J., Zhou C., Long J., Ding Z., Yuan R., Xu C., (2018), Reducing the barrier effect of graphene sheets on a Ag cocatalyst to further improve the photocatalytic performance of TiO_2, *RSC Advances*, **8**, 14056-14063.

Mahmoodi N.M., Khari F.A., Khatibzadeh M., Gharanjig K., (2017), Synthesis of alginate amide composite using microwave and its dye removal ability, *Environmental Engineering and Management Journal*, **16**, 1859-1866.

Nuțescu Duduman C., Gómez De Salazar J.M., Barrena Pérez M.I., Harja M., Palamarciuc I., Gómez De Castro C., (2016), Obtained of nanocomposites: Cu, CuO and $Cu(OH)_2$ - CNF by sol-gel method, *International Journal of Modern Manufacturing Technologies*, **VIII**, 13-18.

Nuțescu Duduman C., Gómez de Salazar y Caso de Los Cobos J.M., Harja M., Barrena Pérez M.I., Gómez de Castro C., Cretescu I., (2018), Preparation and characterization of nanocomposite material based on TiO_2-Ag for environmental applications, *Environmental Engineering and Management Journal*, **17**, 2813-2821.

Qian R., Zong H., Schneider J., Zhou G., Zhao T., Li Y., Pan J.H., (2018), Charge carrier trapping, recombination and transfer during TiO_2 photocatalysis: An overview, *Catalysis Today*, in press, https://doi.org/10.1016/j.cattod.2018.10.053

Ran H., Fan J., Zhang X., Mao J., Shao G., (2018), Enhanced performances of dye-sensitized solar cells based on Au-TiO_2 and Ag-TiO_2 plasmonic hybrid nanocomposites, *Applied Surface Science*, **430**, 415-423.

Rusu L., Harja M., Simion A.I, Suteu D., Ciobanu G., Favier L., (2014), Removal of Astrazone blue from aqueous solutions onto brown peat. Equilibrium and kinetics studies, *Korean Journal of Chemical Engineering*, **31**, 1008-1015.

Sakurai K., Mizusawa M., (2010), X-ray Diffraction Imaging of Anatase and Rutile, *Analytical Chemistry*, **82**, 3519-3522.

Sanzone G., Zimbone M., Cacciato G., Ruffino F., Carles R., Privitera V., Grimald M.G., (2018), Ag/TiO_2 nanocomposite for visible light-driven photocatalysis, *Superlattices and Microstructures*, **123,** 394-402.

Sarina S., Waclawik E.R., Zhu H., (2013), Photocatalysis on supported gold and silver nanoparticles under ultraviolet and visible light irradiation, *Green Chemistry*, **15**, 1814-1833.

Su R., Bechstein R., So L., Vang R.T., Sillassen M., Esbjornsson B., Palmqvist A., Besenbache F., (2011), How the anatase-to-rutile ratio influences the photoreactivity of TiO_2, *The Journal of Physical Chemistry C*, **115**, 24287-24292.

Tobaldi D.M., Pullar R.C., Gualtieri A.F., Seabra M.P., Labrincha J.A., (2013), Sol-gel synthesis, characterisation and photocatalytic activity of pure, W, Ag and W/Ag co-doped TiO_2 nanopowders, *Chemical Engineering Journal*, **214**, 364-375.

Vajda K., Saszet K., Kedves E.Z, Kása Z., Danciu V., Baia L., Magyari K, Hernádi K, Kovács G., Pap Z., (2016), Shape-controlled agglomeration of TiO_2 nanoparticles, New insights on polycrystallinity vs. single crystals in photocatalysis, *Ceramics International*, **42**, 3077-3087.

Van Dillen A.J., Terörde R.J., Lensveld D.J., Geus J.W., De Jong K.P., (2003), Synthesis of supported catalysts by impregnation and drying using aqueous chelated metal complexes, *Journal of Catalysis*, **216**, 257-264.

Waterhouse G.I.N., Bowmaker G.A., Metson J.B., (2001), The thermal decomposition of silver (I, III) oxide: A combined XRD, FT-IR and Raman spectroscopic study, *Physical Chemistry Chemical Physics*, **3**, 3838-3845.

Wetchakun N., Incessungvorn B., Wetchakun K., Phanichphant S., (2012), Influence of calcination temperature on anatase to rutile phase transformation in TiO_2 nanoparticles synthesized by the modified sol–gel method. *Materials Letters*, **82**, 195-198.

Zhao W., Zhang Z., Zhang J., Wu H., Xi L., Ruan C. (2016), Synthesis of Ag/TiO_2/graphene and its photocatalytic properties under visible light, *Materials Letters*, **171**, 182-186.